

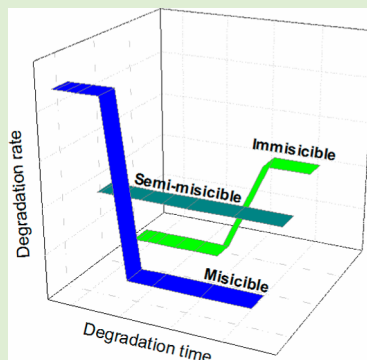
Tuning the Degradation Profiles of Poly(L-lactide)-Based Materials through Miscibility

Veluska Arias, Anders Höglund, Karin Odelius, and Ann-Christine Albertsson*

Department of Fiber and Polymer Technology, KTH Royal Institute of Technology, SE-100 44 Stockholm, Sweden

Supporting Information

ABSTRACT: The effective use of biodegradable polymers relies on the ability to control the onset of and time needed for degradation. Preferably, the material properties should be retained throughout the intended time frame, and the material should degrade in a rapid and controlled manner afterward. The degradation profiles of polyester materials were controlled through their miscibility. Systems composed of PLLA blended with poly[(*R,S*)-3-hydroxybutyrate] (a-PHB) and polypropylene adipate (PPA) with various molar masses were prepared through extrusion. Three different systems were used: miscible (PLLA/a-PHB5 and PLLA/a-PHB20), partially miscible (PLLA/PPA5/comp and PLLA/PPA20/comp), and immiscible (PLLA/PPA5 and PLLA/PPA20) blends. These blends and their respective homopolymers were hydrolytically degraded in water at 37 °C for up to 1 year. The blends exhibited entirely different degradation profiles but showed no diversity between the total degradation times of the materials. PLLA presented a two-stage degradation profile with a rapid decrease in molar mass during the early stages of degradation, similar to the profile of PLLA/a-PHB5. PLLA/a-PHB20 presented a single, constant linear degradation profile. PLLA/PPA5 and PLLA/PPA20 showed completely opposing degradation profiles relative to PLLA, exhibiting a slow initial phase and a rapid decrease after a prolonged degradation time. PLLA/PPA5/comp and PLLA/PPA20/comp had degradation profiles between those of the miscible and the immiscible blends. The molar masses of the materials were approximately the same after 1 year of degradation despite their different profiles. The blend composition and topographical images captured at the last degradation time point demonstrate that the blending component was not leached out during the period of study. The hydrolytic stability of degradable polyester materials can be tailored to obtain different and predetermined degradation profiles for future applications.



INTRODUCTION

Tailoring the degradation rate of poly(L-lactide) (PLLA) has been addressed using several techniques, including copolymerization,^{1–3} plasticization,^{4,5} stereocomplexation,^{6–8} blending,^{9,10} and surface modification.^{11,12} These approaches are generally designed to accelerate the degradation rate of PLLA; however, despite their effectiveness, they suffer from some inherent drawbacks. Copolymerization, stereocomplexation, and surface modification involve relatively complicated synthesis procedures; in addition, they are expensive and time-consuming. The development of a facile and direct method to control PLLA degradation is an important research focus. In general, plasticization is an easy and common method used to improve the flexibility of PLLA. However, plasticization is not always straightforward,¹³ and low molar mass plasticizers might migrate from the polymer matrix. Although lactide is known as a nontoxic and environmentally friendly plasticizer for PLLA, it migrates relatively quickly to the surrounding medium, leaving a stiff material with inferior properties.¹⁴ In addition, controlling the stability of PLLA over time is often more important than accelerating the degradation process. Hydrolytic degradation is influenced by numerous factors, such as the crystallinity, the residual monomer, the impurities, the molar mass, the molar mass distribution, the hydrophobicity, the

molecular architecture, and the size and shape of the sample.¹⁵ Hydrolytic degradation of PLLA was initially observed as a heterogeneous process. During the initial degradation, low-molar-mass compounds are generated both in the bulk and at the surface, whereas only the latter migrates to the surrounding medium. The degradation products in the bulk accumulate and are subsequently released in a burst when the molar mass drops below a certain value.¹⁶ Efforts have been made in an attempt to prevent this burst release. Biodegradable plastics require a long shelf life and a limited degradation time in water, soil, or compost. Obtaining the required degradation rate alongside the necessary mechanical properties is often challenging.

Blending polymers is a simple way to modify the physical and mechanical properties of polymers, as well as their degradability.^{17,18} Aliphatic polyesters, such as poly[(*R,S*)-3-hydroxybutyrate] (a-PHB),^{17,19–21} polypropylene adipate (PPA),^{22,23} poly(butylene adipate-*co*-terephthalate),²⁴ and poly(*ε*-caprolactone),²⁵ have been used as blending materials with PLLA. Unfortunately, the weak or nonexistent secondary interactions between PLLA and other polyesters render most blends

Received: November 11, 2013

Revised: November 26, 2013

Published: November 26, 2013



immiscible. One exception is the fully amorphous a-PHB that is synthesized via the ring-opening polymerization of racemic β -butyrolactone.²⁶ Blends of PLLA and a-PHB are miscible across a range of compositions.^{27,28} The miscibility of PLLA blended with semicrystalline and biodegradable PPA is poor and depends on the molar mass of the PPA.²²

Studies on the degradation of PLLA-based blends have been focused either on the solid-phase structure of the blend during hydrolysis or on the influence of the miscibility on the mechanical properties of the material during degradation. However, controlling the degradation profile of PLLA-based blends through the miscibility between the components without altering the overall degradation time remains unresolved. Our goal was to obtain controlled and predetermined degradation profiles of PLLA-based materials during hydrolytic degradation through the miscibility of PLLA melt-blended with different polyesters. Three different systems were chosen: miscible, partially miscible and immiscible PLLA-based blends with various structures and molar masses of the blending components. We hypothesize that the miscibility between the PLLA and the blending component strongly influences the degradation profiles; specifically, the miscibility is a dynamic function of the degradation time. Through assessment of these changes during degradation, future polyester-based systems with controlled hydrolytic endurance can be designed.

EXPERIMENTAL SECTION

Materials. The monomer L-lactide (Boehringer Ingelheim, France) was purified by recrystallization three times in dry toluene. Ethylene glycol (EG; Sigma-Aldrich, Sweden) and stannous 2-ethylhexanoate ($\text{Sn}(\text{Oct})_2$; 95%, Sigma-Aldrich, Sweden) were used as an initiator and as a catalyst, respectively. Synthetic atactic poly[(R,S)-3-hydroxybutyrate] (a-PHB) was provided by the Polish Academy of Science, Center of Polymer and Carbon Materials, at two different molar masses ($M_n = 5000 \text{ g/mol}$, $M_w/M_n = 1.6$ and $M_n = 20000 \text{ g/mol}$, $M_w/M_n = 1.7$) and was used after being dissolved in chloroform and further precipitated in hexane. Adipic acid (AA; Sigma-Aldrich, Sweden), 1,3-propanediol (Sigma-Aldrich, Sweden), titanium(IV) isopropoxide (TIP; Sigma-Aldrich, Sweden), water for chromatography (Merck, Germany), and the solvents hexane (Fisher Scientific, Sweden), methanol (LC-MS hypergrade Merck, Germany), toluene (Fisher Scientific, Sweden), and chloroform (Fisher Scientific, Sweden) were used as received.

Polymer Synthesis. Poly(L-lactide) (PLLA) was synthesized via the ring-opening polymerization of L-lactide. The initiator was ethylene glycol, and stannous 2-ethylhexanoate [$\text{Sn}(\text{Oct})_2$] was the catalyst. The reaction was stirred continuously at 110 °C for 72 h, in accordance with a previously published procedure.²⁹

Polypropylene adipate (PPA) was synthesized through a stepwise polymerization using adipic acid and 1,3-propanediol as comonomers according to a published procedure.²² We performed the synthesis by adding AA and 1,3-propanediol in a 1:1.2 molar ratio to ensure reaction with the hydroxylated end groups and to achieve a molar mass (M_n) of 5000 g/mol. The polymerization involved two steps. The first step was the direct esterification of the comonomers at 190 °C because the boiling point of 1,3-propanediol is 188 °C. The temperature was held constant until the theoretical amount of water was collected in a cooled trap connected to the vessel. During the second step, the catalyst (TIP) was added in a 1:1000 molar ratio relative to the diacid. The pressure was kept very low to ensure high vacuum, and the temperature was increased to 210 °C. The reaction time was 100 min, and the reaction was performed under an inert atmosphere with continuous stirring. The ratios of the comonomers were varied to tailor the molar mass of the final product. To reach a M_n of 20000 g/mol, AA and 1,3-propanediol were added in a 1:1.05 molar ratio and reacted for 240 min.

The block copolymer PLLA-*co*-PPA was used as a compatibilizer and was synthesized through ring-opening polymerization of L-lactide, with low-molar-mass polypropylene adipate ($M_n = 5000 \text{ g/mol}$) as initiator and $\text{Sn}(\text{Oct})_2$ as catalyst. The reaction time was 48 h under continuous stirring at 110 °C to generate PLLA/PPA (75/25) with a M_n of 20000 g/mol.

Thermogravimetric Analysis (TGA). To minimize degradation during processing, the thermal stabilities of the materials were evaluated using TGA (Mettler Toledo TGA/DSC 1 module). Five milligrams of sample was loaded into a ceramic cup. The samples were heated from 25 to 600 °C at 10 °C/min under nitrogen (nitrogen flow rate of 50 mL/min).

Sample Preparation. The materials were blended using an extrusion process with a twin-screw mini extruder (DSM- Xplore 15 microcompounder, model 2005), with a temperature gradient of 168/168/170 °C from the feed throat to the die, whereas the outlet temperature was 160 °C. The screw speed was 80 rpm for 3 min. Ten grams of material was preblended in 200 mL of chloroform. The solutions were cast in a Petri dish for 1 week to allow the solvent to evaporate. Before being extruded, the samples were dried overnight at 40 °C under vacuum to minimize degradation during processing. The extruded materials were melt-pressed into films with a hot press (Fontijne Presses). Three grams of material was placed in a 15 × 15 cm² mold. The temperature was set to 180 °C, and the melt-pressing was performed under a nitrogen atmosphere for 1 min at 200 kN. Figure 1 shows the molecular structures of the polymers used to

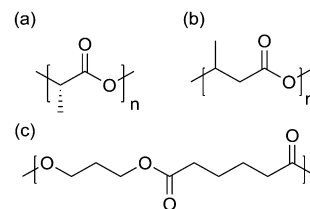


Figure 1. Molecular structures of (a) poly(L-lactide), (b) poly[(R,S)-3-hydroxybutyrate], and (c) polypropylene adipate.

prepare the blends. The blends had a theoretical composition of 90/10% (w/w) PLLA/polyester. The block copolymer PLLA-*co*-PPA was used as a compatibilizer (comp) for the two blends containing PPA with a composition of 89/9/2% (w/w) PLLA/PPA/compatibilizer.

Hydrolysis. Six different PLLA-based blended films and their respective homopolymers were subjected to hydrolytic degradation in 37 °C water for up to 1 year. The mass of each sample was approximately $30 \pm 1 \text{ mg}$, and the melt-pressed films had a round shape with $d = 1 \text{ cm}$ and a thickness of 0.2 mm. The samples were placed in a vial containing 10 mL of water; the vial was sealed with a butyl/PTFE septum and an aluminum lid before being placed in a thermostatically controlled oven. Triplicate samples of each material were withdrawn from the degradation milieu at predetermined times between 1 and 364 days, dried under vacuum for 1 week, and subjected to various analyses. In addition, the water-soluble degradation products in the sample solutions were analyzed after 2 and 24 h of immersion as well as after each hydrolysis process.

Mass Loss. We followed the degradation by measuring the sample mass that remained after each hydrolysis period. After the materials were withdrawn from the degradation medium, they were dried under reduced pressure. We determined the remaining mass by comparing the dry mass of the specimen (m_d) at the specific time with the initial mass of the specimen (m_0), according to eq 1:

$$\text{remaining mass} = \frac{m_d}{m_0} \times 100 \quad (1)$$

Size Exclusion Chromatography (SEC). The molar masses and the polydispersity indices of the starting materials and of the materials after each hydrolysis period were evaluated using a Verotech PL-GPC 50 Plus system equipped with a PL-RI detector and two Mixed-D (300

$\times 7.5 \text{ mm}^2$) columns from Varian. The samples were injected using a PL-AS RT Autosampler for a PLGPC 50 Plus using chloroform as the mobile phase (1 mL/min, 30 °C). Polystyrene standards with narrow molar mass distributions from 580 to 400 000 g/mol were used for calibration. Corrections for the flow rate fluctuations were performed using toluene as an internal standard. The CirrusTM GPC Software was used to process the data. The degradation kinetics were followed by assuming an exponential decrease in M_n according to eq 2:³⁰

$$\ln M_n(t_2) = \ln M_n(t_1) - kt \quad (2)$$

Nuclear Magnetic Resonance (NMR). The structures of the synthesized materials and the compositions of the blends were confirmed using ^1H NMR and ^{13}C NMR. The ^1H NMR and ^{13}C NMR spectra were obtained with a Bruker Advance DPX-400 nuclear magnetic resonance spectrometer operated at 400 MHz. Samples of 10 and 100 mg were dissolved in 1 mL of deuterated chloroform (CDCl_3) in a 5 mm diameter sample tube. Nondeuterated chloroform was used as internal standard ($\delta = 7.26 \text{ ppm}$ and $\delta = 77.0 \text{ ppm}$).

^1H NMR (400 MHz, CDCl_3 , δ): PLA 5.13 (q, 3H, $\text{COCH}_2(-\text{CH}_3)\text{-O}$) and 1.56 (d, 3H, CHCH_3); PPA 4.07 (7, 4H, OCH_2CH_2), 2.26 (s, 4H, COCH_2CH_2), 1.89 (m, 2H, $\text{CH}_2\text{CH}_2\text{CH}_2$), and 1.58 (s, 4H, $\text{CH}_2\text{CH}_2\text{CH}_2\text{CH}_2$); a-PHB 5.21 (q, 1H, CHCH_3), 2.57 (2q, 2H, CH_2CH), and 1.25 (d, 3H, CH_3CH).

Differential Scanning Calorimetry (DSC). The thermal properties of the materials were measured using a differential scanning calorimeter (Mettler Toledo DSC 820 module). Approximately 5 mg of the polymer was encapsulated in 40 μL aluminum crucibles without pins. The following temperature program used was as follows: (I) heat from -20 to 200 °C, (II) cool to -20 °C, and (III) heat again to 200 °C. The heating and cooling rate was 40 °C/min under a nitrogen atmosphere (nitrogen flow rate of 50 mL/min). During the second heating scan, the melting temperatures (T_m) were noted as the maximum value of the melting peaks, whereas the glass-transition temperature (T_g) was determined using the midpoint temperature of the glass transition. When determining the crystallinity of the blends, we assumed that only the PLLA component contributed to the heat of fusion. a-PHB is fully amorphous, and the crystalline regions of the PPA component were difficult to appreciate after being blended. The approximate crystallinity of the blends was calculated according to eq 3:

$$w_c = \frac{\Delta H_f}{\Delta H_f^0} \times 100 \quad (3)$$

where w_c is the degree of crystallinity, ΔH_f is the heat of fusion of the sample, and ΔH_f^0 is the heat of fusion of the 100% crystalline PLLA (93 J/g).³¹

Tensile Testing. The mechanical properties of PLLA and the blends were evaluated using tensile testing. The tensile tests on the melt-pressed films were performed using an INSTRON 5566 module according to standard ASTM D638-10. Strips 5 mm wide and 50 mm long were cut from the melt-pressed films; eight specimens were tested for each material. The measurements were performed with a 500 N load cell at 20 mm/min. The samples were preconditioned at 23 °C and 50% RH for 40 h prior to testing, in accordance with the ASTM D618-08 standard.

Dynamic Mechanical Analysis (DMA). The dynamic mechanical analysis of the blends before the degradation study was performed on a TA Instruments model Q800 dynamic mechanical analyzer operated in tensile mode. The specimens were 8 × 5 mm^2 and 0.2 mm thick. The temperature program proceeded as follows: equilibrate at -100 °C for 5 min before heating to 100 °C at 5 °C/min. The oscillation frequency was maintained at 1 Hz at a constant amplitude of 10.0 μm .

Electrospray Ionization Mass Spectrometry (ESI-MS). The water-soluble products were analyzed using a Finnigan LCQ ion-trap mass spectrometer (Finnigan, San Jose, CA). Methanol (LC-MS hypergrade, Merck, Germany) was added to the samples (2:1 v/v), and the solutions were subsequently infused into the ESI ion source at 5 $\mu\text{L}/\text{min}$ using a syringe pump integrated with the instrument. The LCQ ion source was operated at 5 kV, and the capillary temperature

was set to 175 °C. Nitrogen was used as a nebulizing gas, and helium was used as a dampening and collision gas in the mass analyzer. Positive ion mode was used during all of the analyses.

pH. pH measurements on the degradation medium were performed after each hydrolysis interval using a precalibrated pH-meter equipped with an Ag/AgCl electrode.

Scanning Electron Microscopy (SEM). The morphology of the cross-sectional area of the blends was evaluated with a Hitachi S-4800 scanning electron microscope using an accelerating voltage of 1.5 kV. The samples were mounted on metal studs and were sputter-coated with gold–palladium using a Cressington 208HR sputter-coater unit.

Atomic Force Microscopy (AFM). The PLLA homopolymer and PLLA-based materials were topographically characterized using a Nanoscope IIIa multimode atomic force microscope (Digital Instruments) with a 7850 EV scanner. A silicon-etched probe tip (TAP150, Bruker) with a normal spring constant (k) of 5 N/m and a resonance frequency (f_0) of 150–200 kHz was used to scan the image in tapping mode. The surface of the materials was scanned from 1–2 Hz with a selected maximum sample size (512 × 512 pixels). The very slow scan rate was chosen to avoid sample deformation.

RESULTS AND DISCUSSION

The influence of the miscibility on the degradation profiles of PLLA-based blends was assessed during a hydrolytic degradation in water at 37 °C for up to 364 days. Six different PLLA-based blends (90/10% w/w PLLA/polyester) were prepared: two immiscible blends of PLLA with PPA, two miscible blends of PLLA with a-PHB, and two semimiscible blends of PLLA and PPA with copolymer PLLA-*co*-PPA added as a compatibilizer. The molar masses of the added components were 5000 and 20 000 g/mol. We followed the hydrolytic degradation process of the blends and their respective homopolymers by monitoring the degradation profiles given by the changes in their molar mass and the water-soluble degradation products observed by ESI-MS. In addition, the mass loss, thermal properties, morphology, topography, and pH were determined after each hydrolysis time.

Material Properties Prior to Hydrolysis. The materials used and their properties prior to hydrolysis are presented in Table 1. The names of the materials are marked alongside the theoretical molar mass of the blending material with PLLA. For example, PLLA/PPAS is PLLA blended with PPA with a 5000 g/mol molar mass. The molecular structure of the compatibilizer confirmed that a block structure was obtained (Figure S1, Supporting Information). The thermal stability of the polymers was evaluated by TGA before the polymers were processed to ensure a nondestructive melt blending (Figure S2). The compositions of the blends after being processed were very similar to the feed values. The molar masses of the blending components ensured that two low- and two high-molar-mass polyesters were selected for comparison. The molar masses of the blends after being processed were all in the same range and with a narrow polydispersity index. The size exclusion chromatograms of the blends were also evaluated (Figure S3).

Two miscible, two immiscible, and two semimiscible systems with one or two glass-transition temperatures were confirmed from the thermal properties of the materials (Figure 2). In addition, the dynamic mechanical analysis (DMA) measurements supported the category assigned for each blend (Figure S4). A mixture of a-PHB with PLLA is miscible,³² consistent with the results obtained in this work. However, the miscibility of these two polymers depends on the molar mass of the a-PHB and on the blend composition. Analogously, the blends with PPA are known to be immiscible with PLLA.²² Herein, semimiscible systems were defined as blends with two glass-

Table 1. Characteristics of the Polymers Prior to Hydrolysis

sample id	category	blend composition % (w/w) ^a	M _n (g/mol) ^b	PDI ^b	T _g (°C) ^c	T _m (°C) ^c	w _c (%) ^c	E (MPa) ^d	ε _b (%) ^d
PLLA			146 600 ± 1800	1.1 ± 0.0	58 ± 1	171.1 ± 0.4	42 ± 1	650 ± 170	2.4 ± 0.4
PLLA/PPAS	immiscible	90.6/9.4	110 000 ± 300	1.2 ± 0.0	-47.8 ± 0.1; 52 ± 0.2	172.2 ± 0.6	56 ± 2	500 ± 120	3.0 ± 0.6
PLLA/PPA20	immiscible	91.2/8.8	130 000 ± 600	1.1 ± 0.0	-47.4 ± 0.9; 61.1 ± 0.2	174.4 ± 0.2	42 ± 1	440 ± 70	5 ± 2
PLLA/a-PHB5	miscible	89.8/10.9	116 300 ± 900	1.3 ± 0.0	51 ± 0.0	169.5 ± 0.6	52 ± 4	430 ± 70	52 ± 10
PLLA/a-PHB20	miscible	89.3/10.7	152 700 ± 400	1.2 ± 0.0	55.1 ± 0.3	174.6 ± 0.3	40 ± 3	470 ± 90	11 ± 3
PLLA/PPAS/comp	semimiscible	PPA: 10.4 ^e	127 800 ± 1500	1.2 ± 0.0	-47.3 ± 0.2; 52.5 ± 0.3	171.7 ± 0.4	54 ± 1	440 ± 60	12 ± 5
PLLA/PPA20/comp	semimiscible	PPA: 10.9 ^e	131 500 ± 600	1.1 ± 0.0	-47.3 ± 0.1; 57.5 ± 0.8	171.1 ± 0.2	43 ± 2	530 ± 60	270 ± 80
PPAS			5100 ± 70	1.9 ± 0.0			35.8 ± 0.0		
PPA20			15 000 ± 700	1.7 ± 0.1			39.6 ± 0.6		
a-PHB5			4000 ± 900	1.6 ± 0.1	-6.1 ± 0.4				
a-PHB20			45 000 ± 5000	1.7 ± 0.3	6.6 ± 0.9				
PLLA- <i>co</i> -PPA			11 200 ± 100	1.2 ± 0.0					

^aDetermined by ¹H NMR using δ_{PLLA} 5.13 ppm, δ_{PPA} 4.07 ppm, and δ_{PHB} 2.48 ppm.
^bTotal PPA content from the homopolymer and compatibilizer.

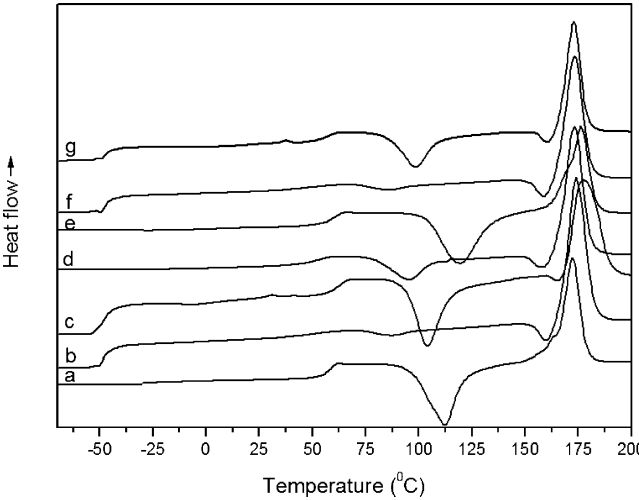


Figure 2. DSC thermograms of the second heating scan of (a) PLLA, (b) PLLA/PPAS, (c) PLLA/PPA20, (d) PLLA/a-PHB5, (e) PLLA/a-PHB20, (f) PLLA/PPAS/comp, and (g) PLLA/PPA20/comp before hydrolysis.

transition temperatures with a decrease in the T_g of PLLA induced by the second component. All of the blends had high melting temperatures and high degrees of crystallinity due to the PLLA component. The degree of crystallinity in the blends with low-molar-mass polyesters was higher than that of the PLLA homopolymer, due to an enhanced packing of the crystalline structure. The miscible and semimiscible blends had a lower Young's modulus (E) and a higher elongation at break (ε_b) than pure PLLA. The PLLA/PPA20/comp blend exhibited the highest E value and the greatest improvement in ε_b (265% extension compared to 2.4% for the PLLA homopolymer). The two blends with PPA and the compatibilizer exhibited significantly improved ε_b values compared to the PPA blends without a compatibilizer, thereby demonstrating that semimiscible blends were obtained.

Degradation Profiles, Molar Mass, and Mass-Loss Changes. The blending of PLLA with a miscible or semimiscible component maintained the polymer properties for a longer period without prolonging the overall degradation time of the material.

The logarithmic M_n profiles were significantly different for all of the investigated materials (Figure 3). The changes in molar mass were used to calculate the hydrolytic degradation rate constants (k) for the PLLA and PLLA blends according to eq 2. The k values were estimated from the logarithmic M_n curves relative to the degradation time (Table S1). The profile of PLLA has two stages, with a rapid decrease during the early degradation time (0–49 days); the k value was 2.8 × 10⁻²(days⁻¹) followed by a slower degradation during the second stage at 0.5 × 10⁻²(days⁻¹). In our previous work regarding the hydrolytic degradation of PLLA in 37 °C water, the first region occurred from 0 and 91 days.³³ The shorter first stage is likely caused by the sample preparation because the PLLA was extruded and melt pressed before hydrolysis, which resulted in a lower degree of crystallinity. The degradation of quenched materials is typically faster due to a facilitated chain relaxation.³⁴

The profile of PLLA/a-PHB5 was similar to that of PLLA, with a degradation rate of 2.3 × 10⁻²(days⁻¹) from 0 to 91 days and 0.5 × 10⁻²(days⁻¹) from 91 to 364 days (Figure 3a). The

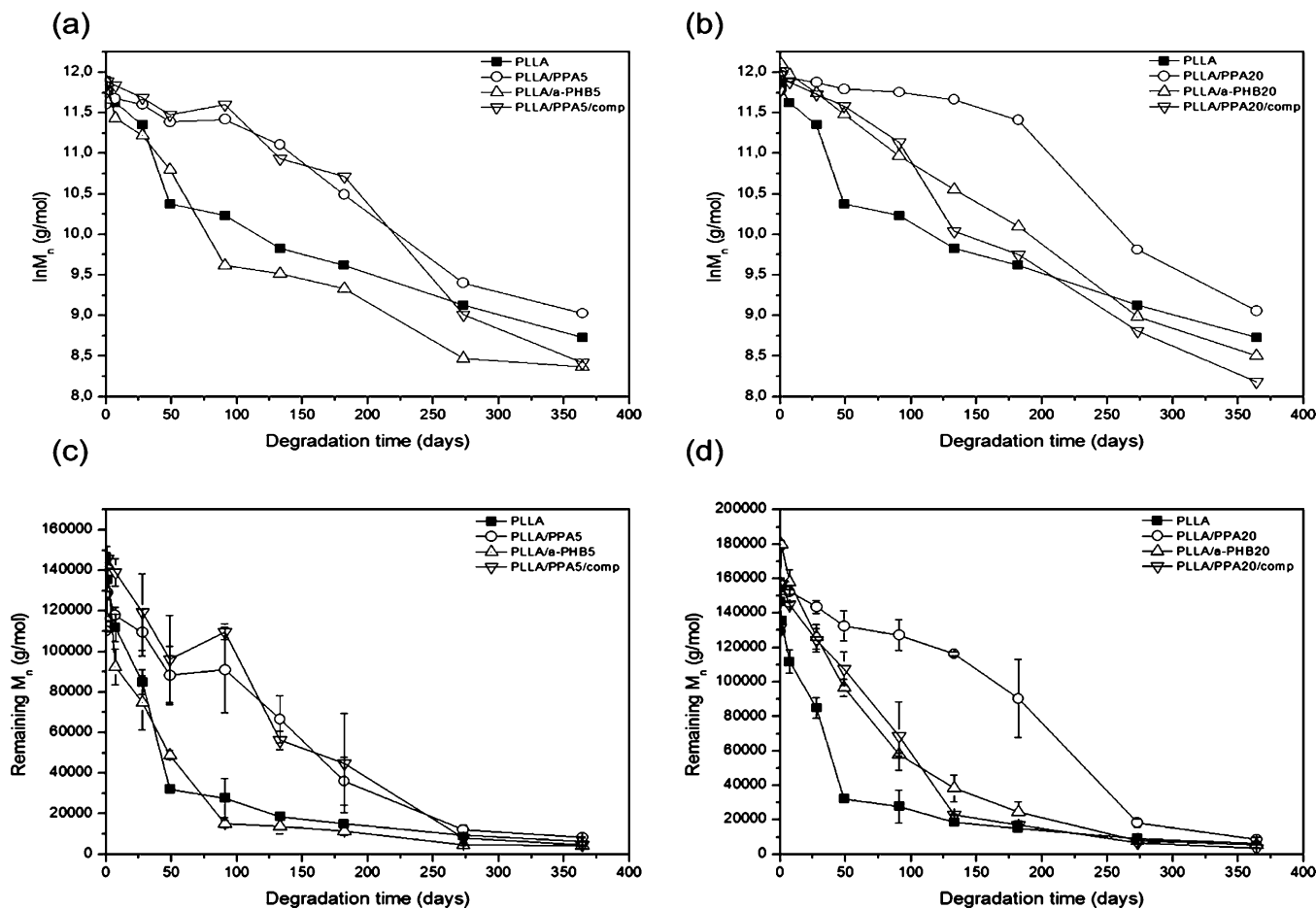


Figure 3. Logarithmic number-average molar mass during the hydrolysis of (a) PLLA and PLLA blends with low-molar-mass polyesters as well as (b) PLLA and PLLA blends with high-molar-mass polyesters. The remaining molar mass during hydrolysis for (c) PLLA and PLLA blends with the low-molar-mass polyesters and (d) PLLA and PLLA blends with high-molar-mass polyesters.

initial degradation of this miscible blend was slightly slower than that of the PLLA homopolymer. However, the PLLA/PPA5 blend showed a two-stage degradation profile with a low k value in the first stage ($0.35 \times 10^{-2}(\text{days}^{-1})$ from 0 to 91 days) and a faster second period ($0.9 \times 10^{-2}(\text{days}^{-1})$). The degradation profile of the PLLA/PPA5/comp blend also showed two stages, with a rapid and prolonged first stage ($0.6 \times 10^{-2}(\text{days}^{-1})$ from 0 to 182 days) and a slower second period ($1.3 \times 10^{-2}(\text{days}^{-1})$). The compatibilizer in the semimiscible PLLA/PPA5/comp blend prolonged the first stage of degradation and reduced the degradation rate relative to the PLLA homopolymer and the immiscible blend PLLA/PPA5.

The degradation profiles of PLLA and its high-molar-mass polyester blends differed significantly (Figure 3b). The PLLA/a-PHB20 blend showed a one-stage degradation profile with a continuous decrease in molar mass over the hydrolysis time and a rate of $1.2 \times 10^{-2}(\text{days}^{-1})$. The profile of PLLA/PPA20 was inverted relative to that of the PLLA homopolymer; the k value was $0.2 \times 10^{-2}(\text{days}^{-1})$ during the longer first degradation stage (0–182 days) and was $1.3 \times 10^{-2}(\text{days}^{-1})$ during the shorter and faster second period. The profile of PLLA/PPA20/comp was similar to that of PLLA, with two stages of degradation: one rapid first stage ($1.3 \times 10^{-2}(\text{days}^{-1})$ from 0 to 133 days) and a slower second stage with a k value of $0.8 \times 10^{-2}(\text{days}^{-1})$. Despite the reduced initial degradation rate of

the semimiscible and immiscible blends, the overall degradation rate of the blends was the same as that of pure PLLA.

The remaining molar mass of the PLLA and PLLA-based blends decreased rapidly over time (Figure 3c,d). The degradation products formed during the hydrolysis of PLLA are not water-soluble until they have a molar mass of ~ 1300 g/mol and therefore remain in the polymer bulk.³⁵ The decrease in molar mass of the blends was slower than that of the PLLA homopolymer; the slowest was the immiscible PLLA/PPA20 blend. However, the miscible PLLA/a-PHB5 blend exhibited a decrease in molar mass similar to that of PLLA. The SEC chromatograms of selected blends (Figure 4) and all materials (Figure S5) illustrate these changes. For clarity, three blends were selected to illustrate the influence of miscibility on the degradation of PLLA blends: the most miscible blend PLLA/a-PHB5 that had a similar degradation profile relative to neat PLLA; the most immiscible blend, PLLA/PPA20, that had an inverted degradation profile compared to that of neat PLLA, and the PLLA/a-PHB20 blend that exhibited intermediate behavior.

Split peaks were observed for PLLA and PLLA/a-PHB5 after 91 days of degradation. The monomodal peak in the SEC chromatograms designate a homogeneous initiation of the ester bond hydrolysis, whereas the bimodal peak is typical for heterogeneous degradation.³⁶ Semicrystalline polyesters undergo heterogeneous degradation because the amorphous regions degrade faster than the crystalline regions. Interestingly, split

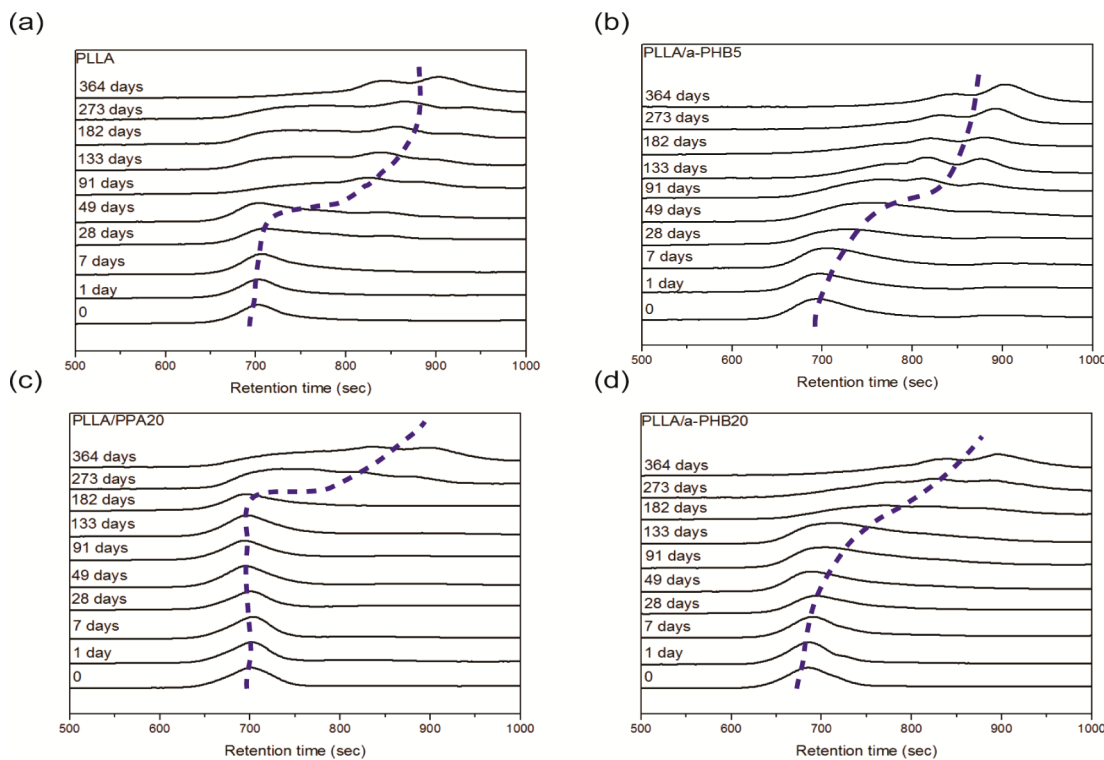


Figure 4. Size exclusion chromatograms of (a) PLLA, (b) PLLA/a-PHB5, (c) PLLA/PPA20, and (d) PLLA/a-PHB20 during hydrolysis.

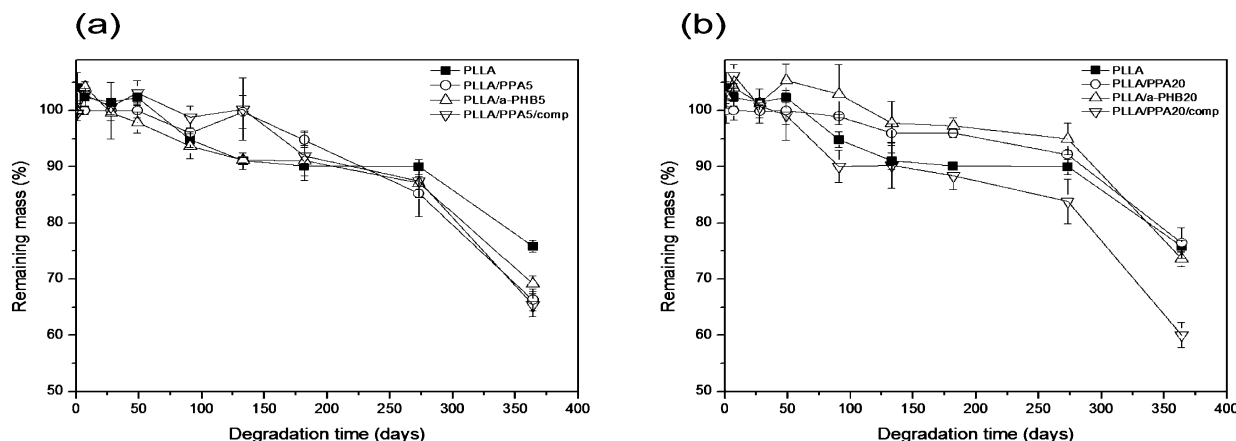


Figure 5. Remaining mass of (a) PLLA and PLLA blends with low molar mass polyesters and (b) PLLA and PLLA blends with high molar mass polyesters during hydrolysis.

peaks were not observed for the PLLA/PPA20 blend until after 273 days, when a sudden broadening occurred. The peak splitting in these three cases correlates to the changes in the degradation profile of these materials (49 days, 91 days and 182 days for PLLA, PLLA/a-PHB5 and PLLA/PPA20, respectively). In contrast to the other blends, the PLLA/a-PHB20 blend showed no abrupt peak broadening, which is consistent with the continuous degradation profile shown in Figure 3.

The mass loss of the blends occurred slowly: after 273 days of degradation, more than 80% mass remained in all cases (Figure 5). As expected, the mass loss was much slower than the reduction in molar mass (cf. Figures 5 and 3). No mass loss was observed during early degradation for any of the blends, proving that the blending component was not leached out immediately upon hydrolysis. This result was also confirmed by NMR data that showed a relatively constant blend composition

throughout the study (Table S2). Despite the different degradation profiles of the blends (Figure 3), the mass loss was approximately the same for the miscible, semimiscible and immiscible systems. The remaining mass of the PPAs and a-PHB5 homopolymers was still greater than 60% after 364 days of hydrolysis, and the corresponding values for PPA20 and a-PHB20 exceeded 80%. Similar to the case of PLLA, these polymers undergo bulk degradation through a hydrolytic scission of the ester linkages that begins immediately upon contact with water, as indicated by the decrease in molar mass (Figure S6).

Degradation Products. The migration of oligomers after each hydrolysis period was analyzed using electrospray ionization mass spectrometry (ESI-MS). Because of the hydrolysis mechanism, the expected oligomers from PLLA, PPA and a-PHB are terminated with hydroxyl and carboxyl

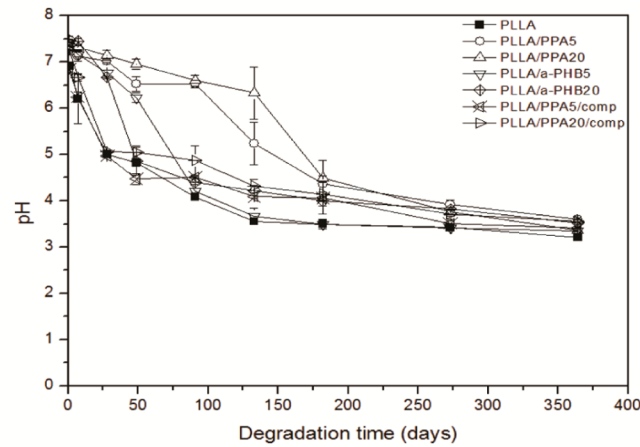
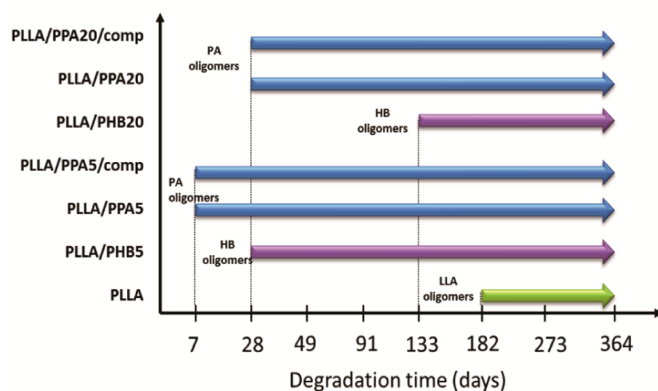


Figure 6. Schematic representation of the appearance of the products formed during the hydrolytic degradation of PLLA and PLLA blends (left). pH as a function of the degradation time during the hydrolysis of PLLA and PLLA blends (right).

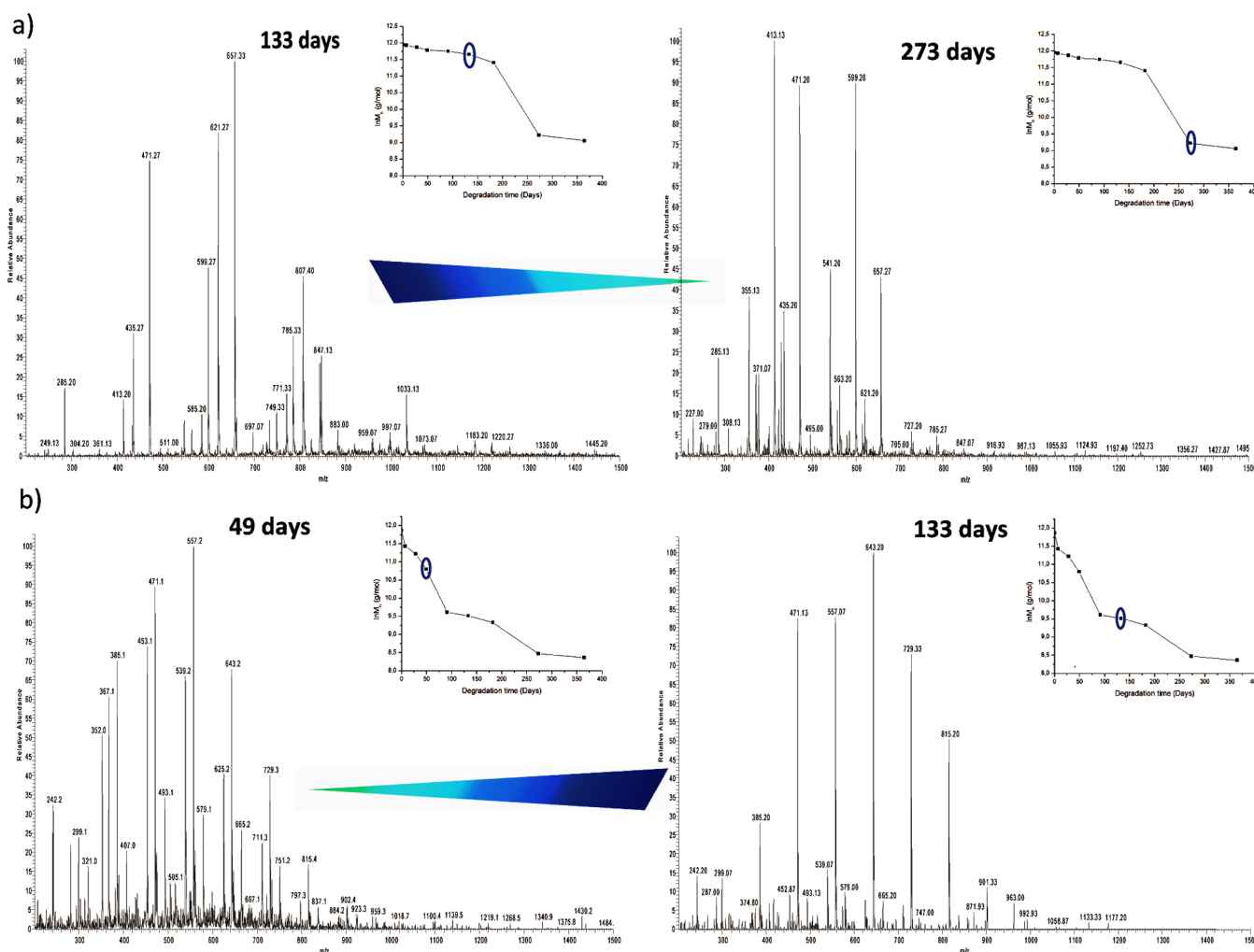


Figure 7. Changes in the degradation product patterns for (a) PLLA/PPA20 during the hydrolysis at 133 and 273 days and (b) PLLA/a-PHB5 during hydrolysis at 49 and 133 days.

end-groups. For the homopolymers, water-soluble oligomers were detected after different hydrolysis periods (Figure S7). For PLLA, water-soluble L-lactide (LLA) oligomers were observed after 182 days. The water-soluble propylene adipate (PA) oligomers from PPAs and PPA20 were detected after 28 and 49 days, respectively, whereas, in the case of a-PHB5 and a-

PHB20, the water-soluble oligomers of hydroxybutyric acid (HB) were observed after 28 and 91 days, respectively.

The oligomeric degradation products from the PLLA-based blends were detected after different degradation times (Figure 6). In all cases, the water-soluble oligomers from the blending component were observed before the PLLA oligomers (Figure

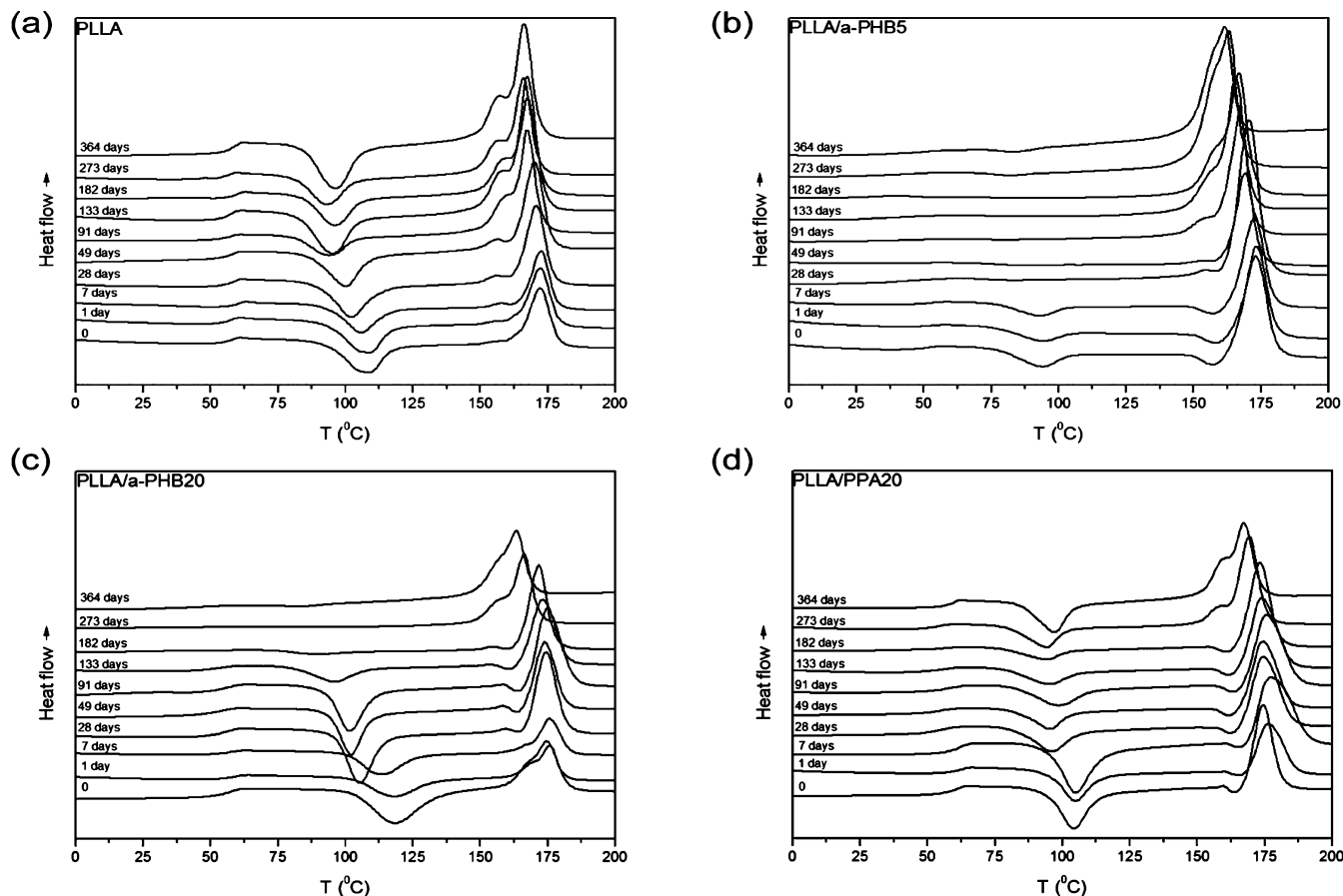


Figure 8. DSC thermograms of the second heating scan of (a) PLLA, (b) PLLA/a-PHB5, (c) PLLA/a-PHB20, and (d) PLLA/PPA20 during hydrolysis.

S8). PLLA/PPAS exhibited PA water-soluble degradation products in the ESI mass spectrum after 7 days of degradation. In contrast, the PLLA/PPA20 blend showed PA water-soluble oligomers after 28 days. For the PLLA/a-PHB5 and PLLA/a-PHB20 blends, only the water-soluble oligomers from the HB repeating unit were observed after 28 and 133 days, respectively. For the PLLA/PPA5/comp and PLLA/PPA20/comp, only PA water-soluble products were observed after 7 and 28 days, respectively. The pH of the degradation medium correlated with the molar mass profiles obtained during an earlier decrease for the PLLA/a-PHB5 products and the latest pH decrease in PLLA/PPA20. The changes in pH were determined to relate the release of acidic products with the differences in the degradation rates (Figure 4). The pH of the PLLA degradation medium decreased after 49 days, although degradation products were detected via ESI-MS after 182 days. The decreased pH is due to the migration of the monomeric degradation product lactic acid. The miscible and semimiscible blends reveal the same trend: a rapid decrease in pH at the beginning, followed by a more gradual decrease. The immiscible systems maintained a neutral pH for a long period, indicating that the presence of PPA inhibited the release of lactic acid products into the medium.

The immiscible components were leached out before the miscible ones: 1) immiscible, 2) semimiscible and 3) miscible. This behavior is due to the better distribution of the a-PHB component in the PLLA matrix that slows down the migration. The HB oligomers from PLLA/a-PHB appeared at the same time point as the PA oligomers from the two PLLA/PPA

blends. One possible reason for this effect is the low molar mass and broad molar mass distribution of the a-PHB5 that facilitates degradation (Table 1).³⁷ The PLLA/a-PHB20 blend showed HB oligomers after a longer time relative to the other blends.

The most miscible (PLLA/a-PHB5) blend and the most immiscible blend (PLLA/PPA20) were selected to demonstrate the degradation product patterns during hydrolysis (Figure 7). The degradation times chosen correspond to before and after the change in the degradation profile for each material (Figure 3). The oligomers from PLLA were observed as a series of peaks with a mass-to-mass peak increment of 72 Da, which corresponds to the molar mass of the LLA repeating unit. These peaks appeared at $m/z = (1 + n \times 72 + 17 + 23)$, which corresponds to the sodium adducts of lactic acid oligomers with hydroxyl and carboxyl end-groups. The series of peaks indicating the a-PHB oligomers appeared with a mass-to-mass peak increment of 86 Da, which corresponds to the molar mass of the HB repeating unit. The sodium adducts of the HB oligomers appeared at $m/z = (1 + n \times 86 + 17 + 23)$. The PPA oligomers were observed as a series of peaks with a mass-to-mass increment of 186 Da, which corresponds to the molar mass of the PA repeating unit. The sodium adducts of PPA appeared at $m/z = (1 + n \times 186 + 75 + 23)$.

The degradation product pattern of PLLA/PPA20 demonstrated the release of larger oligomeric degradation products at the beginning and shifted toward shorter degradation products after prolonged degradation. In contrast, PLLA/a-PHB5 showed larger amounts of shorter degradation products in the first stage, whereas the formation of larger oligomeric

products occurred with increased degradation time. The oligomeric degradation products from a-PHB have been previously studied by ESI-MS, where the series of products appeared at m/z 987, 901, 815, 729, 643, and 557; these products are also observed in Figure 7 and correspond to the a-PHB terminated with hydroxyl and carboxyl end groups.³⁸ The oligomeric degradation products were observed by ESI-MS from PPA as the series of products at m/z 1030, 844, 657, 471, and 285.

Miscibility of the Blends. The miscibility of the selected blends during hydrolysis, specifically the most miscible (PLLA/a-PHB5), the miscible (PLLA/a-PHB20) and the most immiscible (PLLA/PPA20), were investigated using DSC (Figure 8). The PLLA exhibited a slight decrease in the T_g and in the cold crystallization temperature (T_{cc}) as the hydrolysis time increased. The T_g and T_{cc} of the miscible blend (PLLA/a-PHB5) were lower than those of the PLLA before hydrolysis, and the values were difficult to discern after 28 days. The broadening of the T_g peak is common in polymer blends, representing its variation in local compositions. The decreased T_{cc} is related to the decrease in T_g due to degradation and to the widening and suppression of the crystallization range. This second effect is caused by the dispersion of the a-PHB5 component in the matrix because the crystallization process occurs in the homogeneous phase. This phenomenon has previously been observed in PLLA/a-PHB blends.³² The T_g of PLLA/a-PHB20 was lower than that of the PLLA homopolymer, which indicates a partial dispersion of the a-PHB20 component in the PLLA phase. The T_{cc} decreased when the hydrolysis time increased; this change was no longer obvious after 182 days of degradation. Therefore, the miscibility in the melt for this blend increased during hydrolysis, which is related to a decrease in the molar mass of the a-PHB20 component. Notably, the altered degradation profile for PLLA/a-PHB5 occurred after 91 days, coinciding with the last cold-crystallization observation (cf. Figures 3a and 8b). For PLLA/a-PHB20 with a linear degradation profile, a continuous decrease in the cold-crystallization peak with no abrupt change was observed (cf. Figures 3b and 8d). The T_g and T_{cc} of the PLLA component in the immiscible PLLA/PPA20 blend exhibited a similar trend to those of the PLLA homopolymer during hydrolysis. However, a slight broadening of the crystallization peak for PLLA/PPA20 was observed during intermediate degradation.

The T_g and T_{cc} of the immiscible blend PLLA/PPA5 were difficult to discern (Figure S9). This effect has previously been observed in similar blends of PLLA with polybutylene adipate (PBA); the melting peak of PLLA and the glass-transition temperature of PBA were not detectable by DSC because of possible interactions between the two polymers that influenced the crystallization behavior.³⁹ Therefore, some interactions might exist in the PLLA/PPA5 blend that do not exist in the PLLA/PPA20 blend. For the semimiscible blends (PLLA/PPA5/comp and PLLA/PPA20/comp), the thermal curves obtained during hydrolysis showed patterns similar to that for PLLA/PPA5.

The miscibility during hydrolysis was also monitored by atomic force microscopy (AFM), which revealed significant differences in the topography of the selected blends before and after 182 days of hydrolysis. The phase images of PLLA homopolymer and the selected blends, specifically the most miscible PLLA/a-PHB5 and the most immiscible PLLA/PPA20, were captured using tapping-mode imaging (Figure

9); the root-mean-square roughness (R_q) of the surfaces was calculated using three representative topographical images of each material.

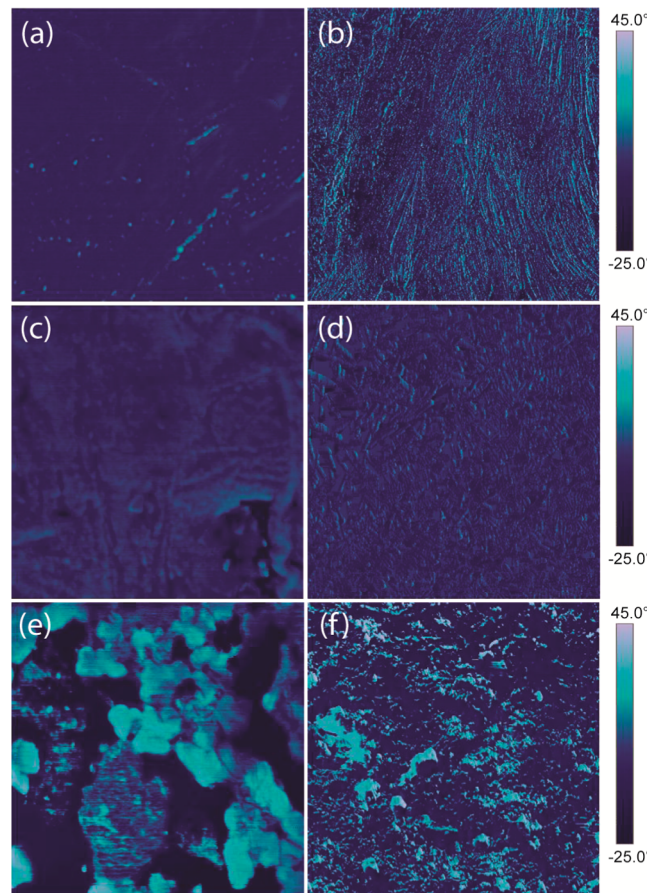


Figure 9. Representative AFM phase images of (a) PLLA before hydrolysis, (b) PLLA after 182 days of hydrolysis, (c) PLLA/a-PHB5 before hydrolysis, (d) PLLA/a-PHB5 after 182 days of hydrolysis, (e) PLLA/PPA20 before hydrolysis, and (f) PLLA/PPA20 after 182 days of hydrolysis. All AFM pictures were scanned over a $5 \times 5 \mu\text{m}^2$ area.

PLLA had one uniform phase before and after hydrolysis. The PLLA/a-PHB5 blend also presented one single phase in the surface images before and after hydrolysis, suggesting that the a-PHB5 domains coalesced in the PLLA matrix. In contrast, PLLA/PPA20 had two separate phases on the surface before and after 182 days of hydrolysis. Compared to the PLLA homopolymer, the elliptical spots represent agglomerations from the PPA20 domains in the PLLA matrix. However, a more dispersed PPA20 domain was observed after 182 days of degradation, indicating the possible miscibility enhancement. The surface roughness before hydrolysis was higher for PLLA/a-PHB5 than for the PLLA homopolymer and PLLA/PPA20: 36 ± 1 , 33 ± 2 , and 26 ± 4 nm, respectively. These differences in the roughness are possibly due to the differences in the crystallinity of the samples (Table 1). All of the samples showed a slight decrease in surface roughness after 182 days of hydrolysis, with values of 24 ± 4 , 32 ± 3 , and 22 ± 3 nm for PLLA, PLLA/a-PHB5, and PLLA/PPA20, respectively. These results indicate that all of the materials underwent bulk degradation and not surface erosion, which is also supported by the large decrease in molar mass after 182 days of degradation (Figure 3).

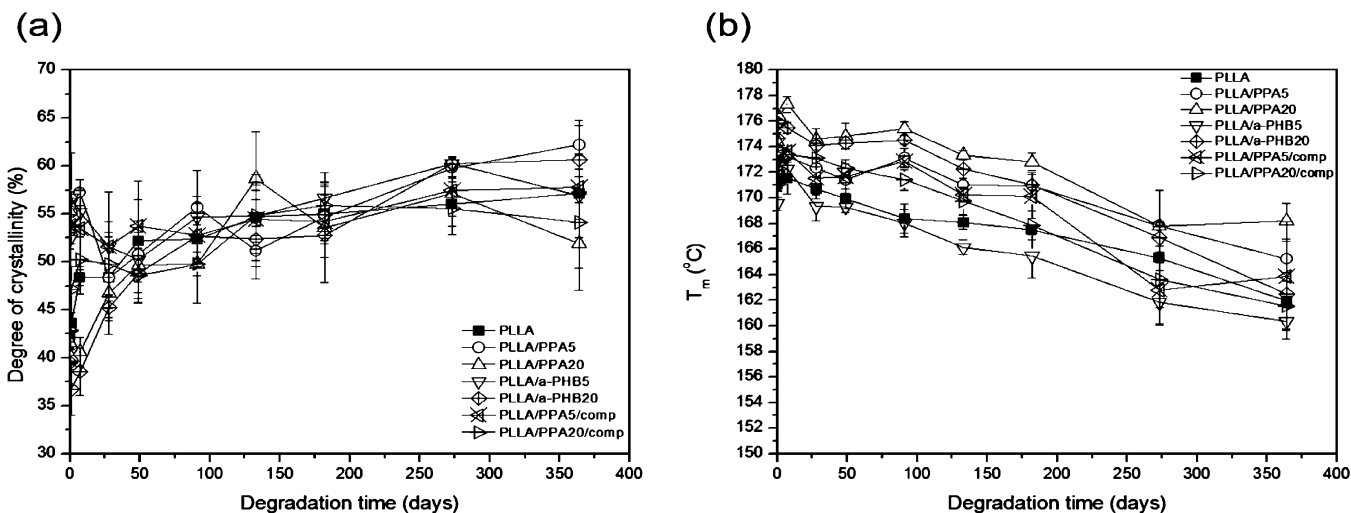


Figure 10. (a) Degree of crystallinity and (b) the melting temperature of the PLLA and PLLA blends during hydrolysis as a function of degradation time.

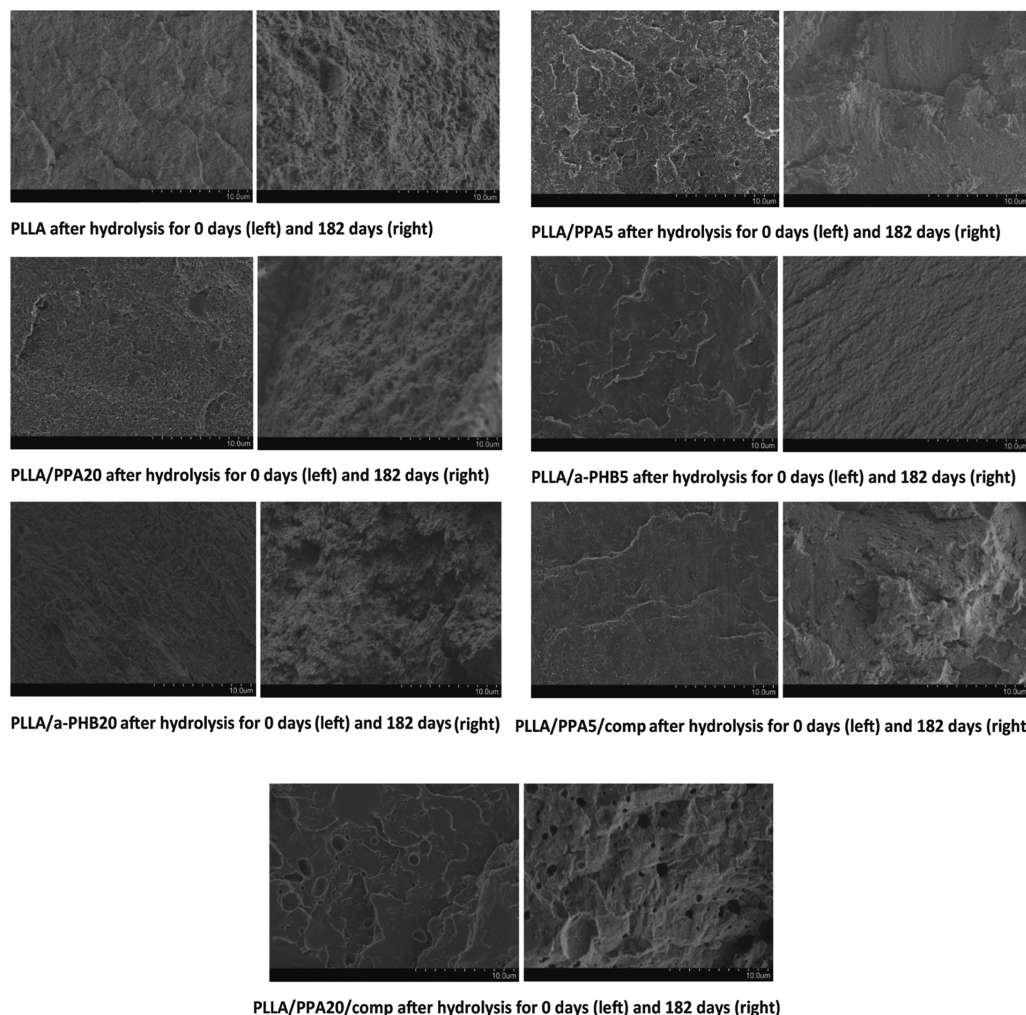


Figure 11. Scanning electron micrographs of the cross-sections of the PLLA and PLLA blends hydrolyzed for 0 and 182 days in H_2O at 37 °C.

Thermal Properties. The effect of hydrolysis on the degree of crystallinity and melting temperature, T_m , was determined using DSC thermograms (Figure 10). The degree of crystallinity for all of the materials increased with increasing

degradation time. The degradation of semicrystalline polyesters begins in the amorphous regions and continues in the crystalline regions when the amorphous parts are almost fully degraded. Similarly, the melting temperature decreased as the

hydrolysis time increased. Shorter polymer chains are formed during hydrolysis, which decreases the T_m due to the higher mobility that allows for reorientation in the crystalline regions. All materials had very similar T_m values before the hydrolysis, and these small differences persisted. Nevertheless, after 364 days of degradation, the blends with the highest and lowest T_m value were PLLA/PPA20 and PLLA/a-PHBS, respectively. This result agrees with the degradation profiles (Figure 3), where the most miscible blend (PLLA/a-PHBS) degraded the fastest, whereas the most immiscible blend (PLLA/PPA20) degraded the slowest. In addition, the shorter chains observed in the degradation product pattern (Figure 7) may correlate to the large decrease in T_m for PLLA/a-PHBS.

Morphology. The morphology of the unaged and degraded materials after 182 days of hydrolysis was studied from the micrographs of the cross-sectional areas of the films (Figure 11).

As expected, the morphologies of the blends were different before and after 182 days of hydrolytic degradation. Before degradation, the PLLA/PPA5 and PLLA/PPA20 blends showed immiscibility between the two components, as indicated by the presence of two phases. The PLLA/a-PHBS and PLLA/a-PHB20 blends appeared to be miscible but retained rough surfaces, thereby confirming the results in Table 1 and the topography images obtained by AFM (Figure 9). The blends with the compatibilizer (PLLA/PPA5/comp and PLLA/PPA20/comp) showed two phases with a porous structure. The porous structure was more pronounced in the PLLA/PPA20/comp due to the larger holes. This porous structure might influence the mechanical properties because this blend showed a lower E modulus and a higher elongation at break compared to the PLLA homopolymer (Table 1). After 182 days of hydrolysis, all of the blends had a very rough cross-sectional area, demonstrating an increase in crystallinity.

CONCLUSIONS

Controlled degradation profiles of PLLA-based blends were successfully obtained using the miscibility between the components. The PLLA/polyester blends varied in molar mass and structure, permitting a comprehensive view of the influence of miscibility on the degradation of PLLA-based materials. The blends exhibited different degradation profiles with no alteration in the total degradation time of the materials. PLLA had a two-stage degradation profile with a rapid first period followed by a slower and continuous second phase. The miscible PLLA/a-PHBS blend had a two-stage degradation profile similar to that of the PLLA homopolymer, whereas the PLLA/a-PHB20 blend had a constant one-stage degradation profile. The immiscible PLLA/PPA5 and PLLA/PPA20 blends exhibited inversed degradation profiles compared to that of PLLA, with a slower first degradation stage and a faster second stage. The semimiscible PLLA/PPA5/comp and PLLA/PPA20/comp blends had degradation profiles that fell between those of the miscible and the immiscible blends. Despite the different degradation profiles, the molar masses of all of the materials were approximately the same after 1 year of degradation. The miscibility of the semimiscible blends increased during degradation, whereas PLLA/PPA20 remained immiscible during hydrolysis. The molar mass of the blended components strongly influenced the degradation profiles. The changes in the degradation profiles correlated with the changes in the thermal properties of the materials. Topographical images of the materials confirmed the miscibility of the blends

and a bulk degradation process. The water-soluble oligomeric degradation products formed from the blends during hydrolysis were detected in the following order: immiscible, semimiscible and miscible blends. The pattern of the degradation products for the immiscible PLLA/PPA20 shifted from longer to shorter degradation products as the degradation time increased, whereas a shift from shorter to longer degradation products was observed for the miscible PLLA/a-PHBS. The blending component was not completely leached from any of the blends during the period of study. Therefore, we have demonstrated that the hydrolytic stability of PLLA-based materials may be customized to obtain a predetermined degradation profile for future applications.

ASSOCIATED CONTENT

Supporting Information

¹H NMR and ¹³C NMR of the PLLA-co-PPA. TGA curves of PLLA, PPA and a-PHB before processing. SEC chromatograms and DMA curves of PLLA and PLLA blends prior hydrolysis. Hydrolytic degradation rate constants and r-squared values of PLLA and PLLA blends during hydrolysis. Blend composition, SEC chromatograms and DSC thermograms of PLLA and PLLA blends during hydrolysis. Molar mass, remaining mass and pH of the homopolymers during hydrolysis. Positive ion ESI-MS spectra of water-soluble degradation products of the homopolymers and PLLA blends at the time of appearance. This material is available free of charge via the Internet at <http://pubs.acs.org/>.

AUTHOR INFORMATION

Corresponding Author

*Tel.: +46-8-790 82 74. Fax: +46-8-20 84 77. E-mail: aila@polymer.kth.se.

Notes

The authors declare no competing financial interest.

ACKNOWLEDGMENTS

The authors acknowledge the Swedish Research Council, VR (Grant ID: A0347801) and the ERC Advance Grant, PARADIGM (Grant Agreement No.: 246776) for their financial support of this work. The authors gratefully acknowledge Professor Marek Kowalcuk for providing the synthetic atactic poly[(*R,S*)-3-hydroxybutyrate] (a-PHB).

REFERENCES

- (1) Mälberg, S.; Höglund, A.; Albertsson, A.-C. *Biomacromolecules* **2011**, *12*, 2382–2388.
- (2) Wanamaker, C. L.; Tolman, W. B.; Hillmyer, M. A. *Biomacromolecules* **2009**, *10*, 443–448.
- (3) Agatemor, C.; Shaver, M. P. *Biomacromolecules* **2013**, *14*, 699–708.
- (4) Höglund, A.; Hakkarainen, M.; Albertsson, A.-C. *Biomacromolecules* **2010**, *11*, 277–283.
- (5) Burgos, N.; Martino, V. P.; Jiménez, A. *Polym. Degrad. Stab.* **2013**, *98*, 651–658.
- (6) Andersson, S. R.; Hakkarainen, M.; Inkinen, S.; Sodergard, A.; Albertsson, A.-C. *Biomacromolecules* **2012**, *13*, 1212–1222.
- (7) Tsuji, H.; Yamamoto, S.; Okumura, A.; Sugiura, Y. *Biomacromolecules* **2009**, *11*, 252–258.
- (8) Rahaman, M. H.; Tsuji, H. *Polym. Degrad. Stab.* **2013**, *98*, 709–719.
- (9) Tsuji, H.; Del Carpio, C. A. *Biomacromolecules* **2002**, *4*, 7–11.
- (10) Focarete, M. L.; Scandola, M.; Dobrzynski, P.; Kowalcuk, M. *Macromolecules* **2002**, *35*, 8472–8477.

- (11) Höglund, A.; Hakkainen, M.; Edlund, U.; Albertsson, A.-C. *Langmuir* **2010**, *26*, 378–383.
- (12) Cairns, M.-L.; Dickson, G. R.; Orr, J. F.; Farrar, D.; Hawkins, K.; Buchanan, F. J. *J. Polym. Degrad. Stab.* **2011**, *96*, 76–83.
- (13) Arias, V.; Höglund, A.; Odelius, K.; Albertsson, A.-C. *J. Appl. Polym. Sci.* **2013**, *130*, 2962–2970.
- (14) Tsuji, H. Hydrolytic Degradation. In *Poly(Lactic Acid): Synthesis, Structures, Properties, Processing, and Applications*; Auras, R., Lim, L. T., Selke, S. E. M., Tsuji, H., Ed.; John Wiley & Sons, Inc.: Hoboken, NJ; New York, 2010; pp 345–381.
- (15) Göpferich, A. *Biomaterials* **1996**, *17*, 103–114.
- (16) Li, S.; Garreau, H.; Vert, M. *J. Mater. Sci.: Mater. Med.* **1990**, *1*, 123–130.
- (17) Kikkawa, Y.; Suzuki, T.; Kanesato, M.; Doi, Y.; Abe, H. *Biomacromolecules* **2009**, *10*, 1013–1018.
- (18) Fukushima, K.; Feijoo, J. L.; Yang, M.-C. *Eur. Polym. J.* **2013**, *49*, 706–717.
- (19) Focarete, M. L.; Scandola, M.; Dobrzynski, P.; Kowalcuk, M. *Macromolecules* **2002**, *35*, 8472–8477.
- (20) Vogel, C.; Wessel, E.; Siesler, H. W. *Biomacromolecules* **2007**, *9*, 523–527.
- (21) Han, L.; Han, C.; Zhang, H.; Chen, S.; Dong, L. *Polym. Compos.* **2012**, *33*, 850–859.
- (22) Odelius, K.; Ohlson, M.; Höglund, A.; Albertsson, A.-C. *J. Appl. Polym. Sci.* **2013**, *127*, 27–33.
- (23) Zhang, H.; Fang, J.; Ge, H.; Han, L.; Wang, X.; Hao, Y.; Han, C.; Dong, L. *Polym. Eng. Sci.* **2013**, *53*, 112–118.
- (24) Jiang, L.; Wolcott, M. P.; Zhang, J. *Biomacromolecules* **2005**, *7*, 199–207.
- (25) Laredo, E.; Grima, M.; Bello, A.; Wu, D. F.; Zhang, Y. S.; Lin, D. P. *Biomacromolecules* **2010**, *11*, 1339–1347.
- (26) Kowalcuk, M.; Adamus, G.; Jedlinski, Z. *Macromolecules* **1994**, *27*, 572–575.
- (27) Focarete, M. L.; Ceccorulli, G.; Scandola, M.; Kowalcuk, M. *Macromolecules* **1998**, *31*, 8485–8492.
- (28) Kikkawa, Y.; Suzuki, T.; Tsuge, T.; Kanesato, M.; Doi, Y.; Abe, H. *Biomacromolecules* **2006**, *7*, 1921–1928.
- (29) Odelius, K.; Plikk, P.; Albertsson, A.-C. *Biomacromolecules* **2005**, *6*, 2718–2725.
- (30) Pitt, C. G.; Zhong-wei, G. *J. Controlled Release* **1987**, *4*, 283–292.
- (31) Fischer, E. W.; Sterzel, H. J.; Wegner, G. *Kolloid Z. Z. Polym.* **1973**, *251*, 980–990.
- (32) Ohkoshi, I.; Abe, H.; Doi, Y. *Polymer* **2000**, *41*, 5985–5992.
- (33) Höglund, A.; Odelius, K.; Albertsson, A.-C. *ACS Appl. Mater. Interfaces* **2012**, *4*, 2788–2793.
- (34) Vert, M.; Mauduit, J.; Li, S. *Biomaterials* **1994**, *15*, 1209–1213.
- (35) Andersson, S. R.; Hakkainen, M.; Albertsson, A.-C. *Biomacromolecules* **2010**, *11*, 3617–3623.
- (36) Grizzi, I.; Garreau, H.; Li, S.; Vert, M. *Biomaterials* **1995**, *16*, 305–311.
- (37) Rychter, P.; Biczak, R.; Herman, B.; Smylla, A.; Kurcok, P.; Adamus, G.; Kowalcuk, M. *Biomacromolecules* **2006**, *7*, 3125–3131.
- (38) Kwiecień, M.; Adamus, G.; Kowalcuk, M. *Biomacromolecules* **2013**, *14*, 1181–1188.
- (39) Zhao, L.; Peng, X.; Liu, X.; Wang, Y.; Qin, S.; Zhang, J. *Polym. J.* **2013**, *45*, 929–937.